Capillarity

Vol. 3, No. 4, p. 56-61, 2020

Original article

Displacement behavior of methane in organic nanochannels in aqueous environment

Jingjing Huai[1], Zhang Xie[1], Zheng Li[2], Gang Lou[1], Jun Zhang[1], Jianlong Kou[1]*, Hui Zhao[3]*

[1]*Institute of Condensed Matter Physics, Zhejiang Normal University, Jinhua 321004, P. R. China*

[2]*School of Petroleum Engineering, China University of Petroleum (East China), Qingdao 266580, P. R. China*

[3]*School of Petroleum Engineering, Yangtze University, Wuhan 430100, P. R. China*

Keywords:
Molecular dynamics simulation
gas-water interaction
organic nanochannel

Cited as:
Huai, J., Xie, Z., Li, Z., Lou, G., Zhang, J., Kou, J., Zhao, H. Displacement behavior of methane in organic nanochannels in aqueous environment. *Capillarity*, 2020, 3(4): 56-61, doi: 10.46690/capi.2020.04.01.

Abstract:
Shale is rich in organic nanopores where shale gas mainly resides. Shale gas development is often accompanied by water, so studying interactions of gas and water in organic nanopores has become an important topic. Here, we performed molecular dynamics simulations to study the interaction of gas and water in organic nanochannels. It was found that water molecules in the nanochannel could be displaced by methane molecules. And the entered methane molecules would exhibit different layered structures. The above phenomenon is attributed to the fact that methane molecules have lower potential of mean force than water molecules in nanochannels. The revealed mechanism of displacing water molecules with methane molecules in organic nanochannels provides an insight into the interaction of water molecules and methane molecules in organic nanochannels and has tremendous potentials in the development of shale gas.

1. Introduction

The increase demand of resources and the dwindling of conventional resources make the attention of resources development transfer to unconventional resources. With the progress of horizontal drilling and multi-stage hydraulic fracturing technologies (Gregory et al., 2011; Yethiraj and Striolo, 2013), it is possible to exploit unconventional energy with wide distribution and great development potential. At present, the exploitation of unconventional resources has made it an important supplement to conventional resources (Kerr, 2010; Yao et al., 2013). Shale gas, an important unconventional resource, has received extensive attention due to its large reserves (Vidic et al., 2013; Striolo and Cole, 2017; Mayfield et al., 2019).

The pore structure of shale gas reservoirs are complex. There are not only a large number of nanoscale pores, but also micro-scale fractures, resulting in multiscale features in shale gas reservoirs (Loucks et al., 2009; Clarkson et al., 2013; Sun et al., 2017; Liu and Ostadhassan, 2019). As the pore becomes smaller approaching to the nanometer, the interfacial force increases, and the gas confined in the nanopores will show different behaviors from those at the macroscale, which results in the different properties of unconventional resource compared with conventional resource (Zhao et al., 2014a). In addition, the hydraulic fracturing is the key and necessary technology to realize the commercial exploitation of shale gas (Gregory et al., 2011; Yethiraj and Striolo, 2013). The use of hydraulic fracturing means that water will exist in the whole exploitation process, which leads to more complex behaviors of gas in nanopores. It has been proved that pure water in nanochannels shows many different and complex characteristics, such as the resonance behavior, the gating effect and the unusual phase transition (Koga et al., 2001; Beckstein and Sansom, 2003; Li et al., 2007; Kou et al., 2014).

Actually, there are always interactions of gas, water and organic matter during the development of shale gas in water environments (Chalmers and Bustin, 2010). Thus, it is necessary to study the interaction between gas and water in the organic nanochannels (Li et al., 2016, 2017a; Shen et al., 2019). Although the phase change, the occurrence state and the flow mechanism of water/gas molecules in nanopores have been the research hotspots in natural science and many engineering fields (Hummer et al., 2001; Dammer and Lohse, 2006; Bai and Zeng, 2012; Zhao et al., 2014b, 2015; Kou et al., 2015; Lee and Aluru, 2015; Wang et al., 2016; Li et al., 2019a, 2019b). In view of the particularity of shale pore structure

Yandy Scientific Press

*Corresponding author.
E-mail address: huaijj123456@163.com (J. Huai); xz1574736141@163.com (Z. Xie); lzdyx361@163.com (Z. Li); lougang@zjnu.cn (G. Lou); zjungg@yeah.net (J. Zhang); kjl@zjnu.cn (J. Kou); zhaohui@yangteu.edu.cn (H. Zhao).

Received September 30, 2020; revised October 10, 2020; accepted October 10, 2020; available online October 12, 2020.

and reservoir property, the research on gas in confined space in petroleum engineering field is still very limited. Especially when considering the existence of water, due to the limitations of experiments, it is still unable to give a detailed microscopic mechanism. However, it is of great significance to carry out the research on the water-gas interaction in the nanochannels for the efficient exploitation of unconventional gas.

Here, we perform molecular dynamics simulations to investigate the displacement behavior of methane in organic nanochannels in aqueous environment. We found that the water molecules in nanochannels could be spontaneously displaced by methane molecules. In different nanochannels, the entered methane molecules showed a variety of distribution forms. By calculating the equilibrium potentials of mean force of molecule, we revealed the physical mechanism of displacing methane molecules by water molecules in organic nanochannels.

2. Methodology and simulation details

2.1 Model

Organic nanopores are the important storage space of shale gas (Loucks et al., 2009; Clarkson et al., 2013). However, it is difficult to discuss the interaction between water and gas in the organic matter pores due to the complexity of the real structure of organic matters (Mosher et al., 2013; Gu et al., 2015; Jin and Firoozabadi, 2015; Bousige et al., 2016; Li et al., 2017b). Here, the carbon-based nanochannel is adopted to represent the organic nanopore. A nanochannel with a separation of H was prepared. The width (H) of the nanochannel is measured as the distance between the innermost carbon-based layers. The size of the carbon-based layer is 2.8×3.3 nm^2 ($x \times y$). To prevent the influence of the molecules outside the nanochannel on the molecules in the nanochannel, four single-layer graphenes sheets with the same width in the x direction were placed at the two ends of nanochannel. Those graphenes sheets are perpendicular to the nanochannel, the space is divide into three parts. All the carbon atoms of graphene are frozen in their original positions. The simulation configuration is shown in Fig. 1(a). All pictures were shown using the VMD molecular visualization program (Humphrey et al., 1996).

2.2 Simulation method

The Gromacs 4.0.7 molecular dynamics program was used to perform all simulations in the NP_zT ensemble (Hess et al., 2008). The pressure was controlled by Parrinello-Rahman scheme to 1.0 bar with a compressibility coefficient of 4.5×10^{-5} bar^{-1} (Nose and Klein, 1983). In all simulations, the V-rescale thermostat was applied to maintained environment temperature at 300 K (Bussi et al., 2007). TIP3P water model was used (Berendsen et al., 1987). The carbon atoms of all graphene sheets were considered as uncharged Lennard-Jones (LJ) atoms, and the potential parameters for carbon atoms were σ_{CC} = 0.34 nm and ε_{CC} = 0.23 kJ·mol^{-1}, respectively (Bhethanabotla and Steele, 1987). Methane molecule was described using the five-site model (Kaminski et al., 1994), the potential parameters of LJ and Coulomb for the methane molecules were taken from Reference (Kaminski et al., 1994). LJ parameters between different atoms were described by using the Lorentz-Berthelot mixing rules. A cut-off distance of 1.4 nm is used for the LJ potential. The long-range electrostatic interaction was treated by using the particle-mesh Ewald method with a cut-off distance of 1.4 nm. A Fast Fourier transform grid spacing is 0.12 nm. The periodic boundary conditions in three directions were used.

2.3 Potential of mean force profiling

A umbrella sampling method was used to calculate the Potential of Mean Force (PMF) for methane molecule and water molecule (Torrie and Valleau, 1977; Kumar et al., 1995; Roux, 1995). Along the x direction, a point was selected every 0.05 nm, a total of 50 points were selected (because of the symmetry, we chose half of the system). A harmonic fore with an elastic constant of 5000 kJ·mol^{-1}·nm^{-2} was used to keep the molecule at a fixed position in the x direction. For every condition, the system was equilibrated for 2 ns first, then run for 5 ns.

3. Results and discussion

A nanochannel of 0.8 nm in thickness was prepared. Initially, methane molecules were evenly placed in both sides of graphene, then the region including the location of methane and the nanochannel was filled with water molecules, as shown in Fig. 1(a). A 10 ns-simulation was performed. It is found that all the water molecules in the nanochannel are displaced, and the nanochannel is occupied by methane molecules, as shown in Fig. 1(b). To quantitatively observe the number of water molecules and gas molecules in the nanochannel, we calculated the number of water molecules and methane molecules in the nanochannel with the time evolution, as indicated in Fig. 1(c). For counting the number of molecules in the nanochannel, we tracked the positions of the mass centers of water and methane molecules. If the mass center of molecule is in the nanochannel, the molecule is in the nanochannel. It can be seen clearly from Fig. 1(c) tn the first 1.5 ns that the number of water molecules in the nanochannel decreases significantly, and all water molecules completely leaves the nanochannel eventually with the simulation time. As the water molecules break away from the nanochannel, methane molecules enter the nanochannel and finally occupy the nanochannel. The whole process takes only 1 ns. As shown in the enlarged drawing of the initial stage of evolution in Fig. 1(c), the number of water molecules in the nanochannel is almost unchanged in the first 0.2 ns. The molecular visualization program was used to trace simulation snapshots. During this time, methane molecules gradually approached the entrance of the nanochannel. Once some methane molecules enter the nanochannel, other methane molecules will surge up and occupy the whole nanochannel in a short time. Generally, there are two processes for methane molecules to enter the nanochannel. In the first step, methane molecules in the aqueous solution approach the nanochannel by diffusion. In

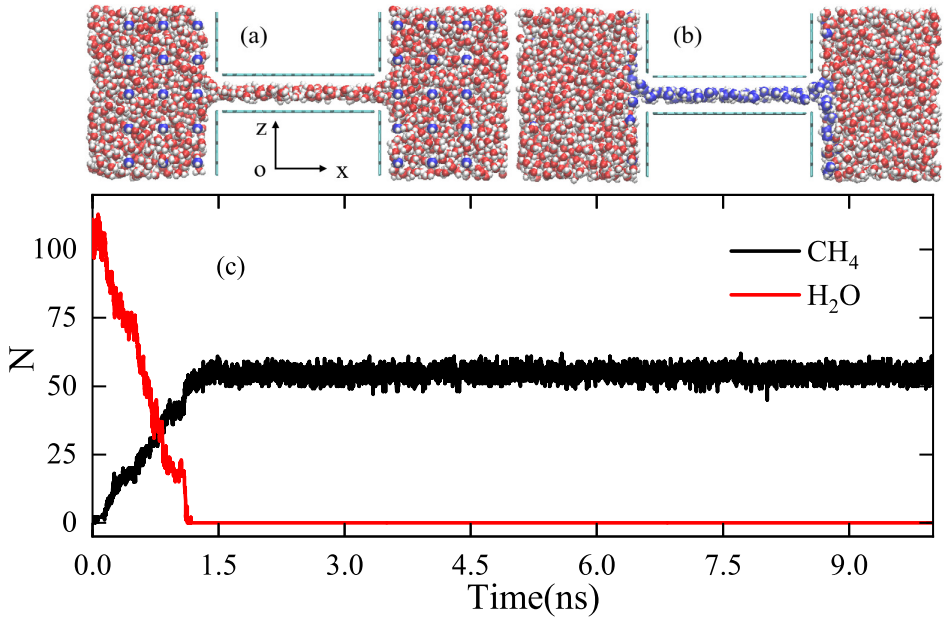

Fig. 1. (a) the initial configurations, (b) snapshot of simulation at t = 10 ns, and (c) the numbers (N) of methane molecules (CH_4) and water molecules (H_2O) as a function of time. The graphene molecule is shown with dark grey. The water molecules are described by spheres with oxygen in red and hydrogen in white, and the methane molecules with carbon in blue and the hydrogen in white.

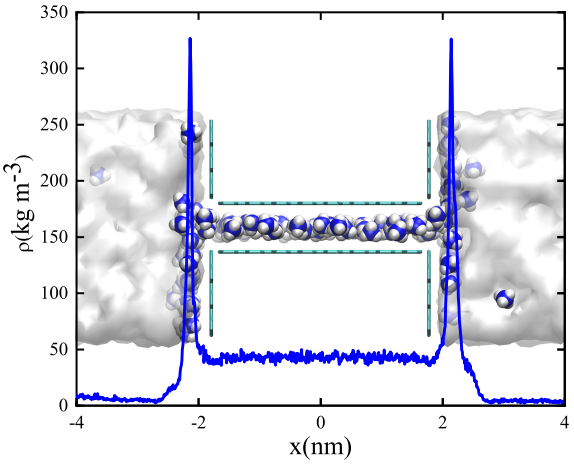

Fig. 2. Density profiles of methane in x direction. Insert is a schematic diagram of the distribution of methane and water molecules in nanochannel. Liquids like clouds are water molecules. Graphene and methane are shown in accordance with Fig. 1.

the second step, methane molecules interact with water molecules in the nanochannel, enter and occupy the nanochannel finally.

We calculated the density distribution of methane molecules in the x direction under steady state, as shown in Fig. 2. It is found that the gas density in the solution is very small, but there is a high peak near the entrance of the slit, and the density is 5-6 times larger than in the nanochannel. In the water environment, a part of methane molecules enter the nanochannel, and more gas molecules accumulates at the end of the nanochannel forming accumulated gas on the surface. This gas accumulation is due to the competition between water-water interaction and water-gas interaction (Li et al., 2019b). The hydrogen bond interaction between water molecules is much larger than the van der Waals interaction between water and gas, resulting in the gas being discharged from the aqueous solution and accumulating on the solid interface, a high density at the solid interface at the entrance of the nanochannel (Li et al., 2019b). The gas density distribution in the nanochannel is unchanged, which is consistent with the change trend of gas molecules in Fig. 1(c). After 1 ns, all water molecules are displaced by gas molecules, forming a stable gas layer in the nanochannel.

To find out why methane molecules can displace water molecules, we computed equilibrium PMF (Torrie and Valleau, 1977; Kumar et al., 1995; Roux, 1995) distribution of the methane and the water, as indicated in Fig. 3. Due to the symmetry of the simulation system, we given the PMF of both the methane molecule and the water molecule on the left half of simulation system. Reference locations with PMF of zero are defined at both ends of the reservoir. The PMF of both the methane molecule and the water molecule far away from the interface are around zero and are nearly constant. The PMF of both the methane molecule and the water molecule decrease rapidly near the interface, and the PMF achieves a minimum. It means that either water or methane molecules prefer to accumulate at the interface. It is noted that methane molecule has a lower PMF than that of water molecule. This means that the methane molecule more prefer to accumulate at the interface than that of water molecule. Within the nanochannel, the PMF of water and methane molecules at the entrance increases significantly. This means that the molecules just entering the nanochannel are not stable, and the PMF of gas molecules is always lower than that of water molecules. The PMF of water molecule in the nanochannel is always higher than that near the entrance. The relatively lower PMF of

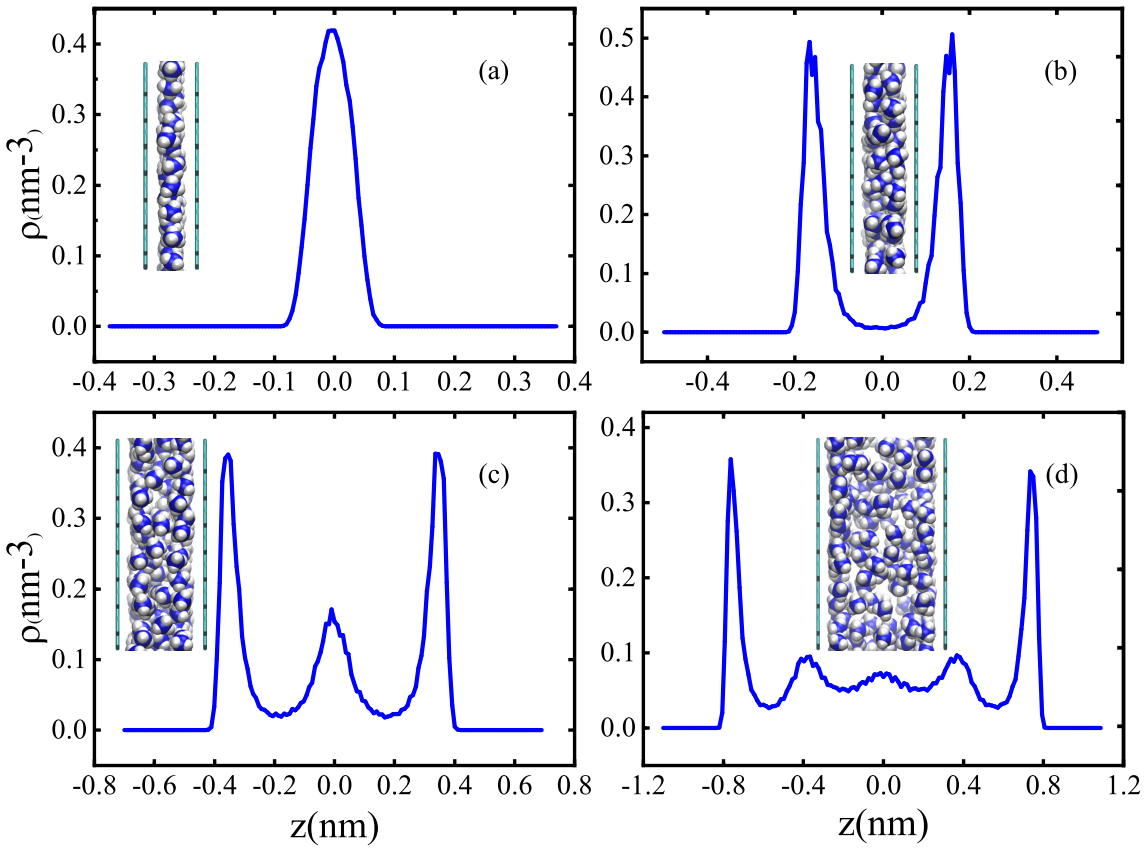

Fig. 4. Density distribution of methane along z axis in nanochannel, (a) H = 0.75 nm, (b) H = 1.0 nm, (c) H = 1.4 nm, and (d) H = 2.2 nm. The insets show snapshots of the distribution of methane molecules in the nanochannels in different widthnesses.

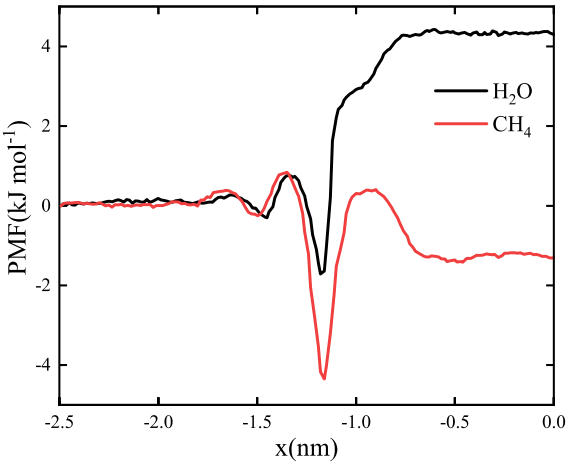

Fig. 3. PMF distribution of water (H_2O) and methane (CH_4) in x direction.

molecules serves to allow molecules to enter the nanochannel more easily. When the both molecules completely enter the nanochannel, the PMF of water molecules continues to increase and reach a stable value, while the gas molecules decrease and reach the minimum value. It is noted that the final PMF of water molecule is higher than that of gas in the nanochannel. The lower PMF of methane molecules promotes methane molecules entering the nanochannel more easily. Therefore, the water molecules can be replaced by methane molecules, which is consistent with the previous findings. This should be the reason why the water molecules can be displaced out of the nanochannel by the methane molecules.

To check the reliability of the nanochannel, we further performed molecular dynamics simulations of nanochannel with different widths in the same way as above. The water molecules in the nanochannel exhibits a similar displacement behavior with methane molecules, indicating the robustness of the demonstrated trend of methane displacement. Fig. 4 illustrates the distribution of methane density in the nanochannel. The nanochannels with different widths show different methane distribution states. Especially, the methane molecules exhibit a monolayer structure for the width of 0.75 nm, the methane molecules exhibit a symmetrical double-layer structure for the width of 1.0 nm, as shown in Figs. 4(a) and 4(b). When the spacing of nanochannel increases to 1.4 nm, the molecular density of two-layer methane decreases, and a layer of methane structure appears in the middle, as shown in Fig. 4(c). When the pore size is larger, the high density still exists near the interface, but the density distribution of methane in the middle becomes gentler, as shown in Fig. 4(d).

4. Conclusions

We studied the gas-water interaction in organic nanochannels by using molecular dynamics simulations. It is shown that methane molecules will come near to the organic interface

in aqueous environments spontaneously, enter the nanochannels, and arrange different gas layer structures. The water molecules in the nanochannels are completely discharged. The phenomenon of gas molecules displacing water molecules in nanochannels is attributed to the lower free energy of gas molecules than that of water molecules. This work reveals a displacement mechanism of gas molecules in the aqueous solutions, and can understand the occurrence characteristics of shale gas in nanochannels and provide a new idea for shale gas recovery.

Acknowledgement

This work was supported partly by the Zhejiang Provincial Natural Science Foundation of China (No. R21A020004), and the National Natural Science Foundation of China (No. 11774313).

Conflict of interest

The authors declare no competing interest.

References

Bai, J., Zeng, X.C. Polymorphism and polyamorphism in bilayer water confined to slit nanopore under high pressure. Proc. Natl. Acad. Sci. USA 2012, 109(52): 21240-21245.

Beckstein, O., Sansom, M.S.P. Liquid-vapor oscillations of water in hydrophobic nanopores. Proc. Natl. Acad. Sci. USA 2003, 100(12): 7063-7068.

Berendsen, H.J.C., Grigera, J.R., Straatsma, T.P. The missing term in effective pair potentials. J. Phys. Chem. 1987, 91(24): 6269-6271.

Bhethanabotla, V.R., Steele, W.A. Molecular dynamics simulations of oxygen monolayers on graphite. Langmuir 1987, 3(4): 581-587.

Bousige, C., Ghimbeu, C.M., Vix-Guterl, C., et al. Realistic molecular model of kerogen's nanostructure. Nat. Mater. 2016, 15: 576-583.

Bussi, G., Donadio, D., Parrinello, M. Canonical sampling through velocity rescaling. J. Chem. Phys. 2007, 126(1): 014101.

Chalmers, G.R., Bustin, M.R. The effects and distribution of moisture in gas shale reservoir systems. Presentation at AAPG Annual Convention and Exhibition, New Orleans, Louisiana, 11-14 April, 2010.

Clarkson, C.R., Bustin, S., Bustin, R.M. Pore structure characterization of North American shale gas reservoirs; using USANS/SANS, gas adsorption, and mercury intrusion. Fuel 2013, 103: 606-616.

Dammer, S.M., Lohse, D. Gas enrichment at liquid-wall interfaces. Phys. Rev. Lett. 2006, 96(20): 206101.

Gregory, K.B., Vidic, R.D., Dzombak, D.A. Water management challenges associated with the production of shale gas by hydraulic fracturing. Elements 2011, 7(3): 181-186.

Gu, X., Cole, D.R., Rother, G., et al. Pores in marcellus shale: A neutron scattering and FIB-SEM study. Energy Fuels 2015, 29(3): 1295-1308.

Hess, B., Kutzner, C., Spoel, D.V.D., et al. GROMACS 4: Algorithms for highly ecient, load-balanced, and scalable molecular simulation. J. Chem. Theory Comput. 2008, 4(3): 435-447.

Hummer, G., Rasaiah, J.C., Noworyta, J.P. Water conduction through the hydrophobic channel of a carbon nanotube. Nature 2001, 414: 188-190.

Humphrey, W., Dalke, A., Schulten, K. VMD: Visual molecular dynamics. J. Mol. Graph. 1996, 14(1): 33-38.

Jin, Z., Firoozabadi, A. Flow of methane in shale nanopores at low and high pressure by molecular dynamics simulations. J. Chem. Phys. 2015, 143(10): 104315.

Kaminski, G., Duffy, E.M., Matsui, T., et al. Free energies of hydration and pure liquid properties of hydrocarbons from the OPLS all-atom model. J. Phys. Chem. 1994, 98(49): 13077-13082.

Kerr, R.A. Natural gas from shale bursts onto the scene. Science 2010, 328(5986): 1624-1626.

Koga, K., Gao, G.T., Tanaka, H., et al. Formation of ordered ice nanotubes inside carbon nanotubes. Nature 2001, 412: 802-805.

Kou, J.L., Lu, H., Wu, F., et al. Electricity resonance-induced fast transport of water through nanochannels. Nano Lett. 2014, 14(9): 4931-4936.

Kou, J.L., Yao, J., Lu, H.J., et al. Electromanipulating water flow in nanochannels. Angew. Chem. Int. Ed. 2015, 54(8): 2351-2355.

Kumar, S., Rosenberg, J.M., Bouzida, D., et al. Multidimensional free-energy calculations using the weighted histogram analysis method. J. Comput. Chem. 1995, 16(11): 1339-1350.

Lee, J., Aluru, N.R. Mechanistic analysis of gas enrichment in gas-water mixtures near extended surfaces. J. Phys. Chem. C 2015, 115(35): 17495-17502.

Li, J., Gong, X., Lu, H., et al. Electrostatic gating of a nanometer water channel. Proc. Natl. Acad. Sci. USA 2007, 104(10): 3687-3692.

Li, J., Li, X., Wu, K., et al. Water sorption and distribution characteristics in clay and shale: Effect of surface force. Energy Fuels 2016, 30(11): 8863-8874.

Li, J., Li, X., Wu, K., et al. Thickness and stability of water film confined inside nanoslits and nanocapillaries of shale and clay. Int. J. Coal Geol. 2017a, 179: 253-268.

Li, Z., Liu, D., Cai, Y., et al. Multi-scale quantitative characterization of 3-D pore-fracture networks in bituminous and anthracite coals using FIB-SEM tomography and X-ray μ-CT. Fuel 2017b, 209: 43-53.

Li, Z., Yao, J., Kou, J. Mixture composition effect on hydrocarbon-water transport in shale organic nanochannels. J. Phys. Chem. Lett. 2019a, 10(15): 4291-4296.

Li, Z., Yao, J., Ren, Z., et al. Accumulation behaviors of methane in the aqueous environment with organic

matters. Fuel 2019b, 236: 836-842.

Liu, K., Ostadhassan, M. The impact of pore size distribution data presentation format on pore structure interpretation of shales. Adv. Geo-Energy Res. 2019, 3(2): 187-197.

Loucks, R.G., Reed, R.M., Ruppel, S.C., et al. Morphology, genesis, and distribution of nanometer-scale pores in siliceous mudstones of the Mississippian Barnett Shale. J. Sediment. Res. 2009, 79(12): 848-861.

Mayfield, E.N., Cohon, J.L., Muller, N.Z., et al. Cumulative environmental and employment impacts of the shale gas boom. Nat. Sustain. 2019, 2: 1122-1131.

Mosher, K., He, J., Liu, Y., et al. Molecular simulation of methane adsorption in micro- and mesoporous carbons with applications to coal and gas shale systems. Int. J. Coal Geol. 2013, 109-110: 36-44.

Nose, S., Klein, M.L. Constant pressure molecular dynamics for molecular systems. Mol. Phys. 1983, 50(5): 1055-1076.

Roux, B. The calculation of the potential of mean force using computer simulations. Comput. Phys. Commun. 1995, 91(1-2): 275-282.

Shen, W., Li, X., Cihan, A., et al. Experimental and numerical simulation of water adsorption and diffusion in shale gas reservoir rocks. Adv. Geo-Energy Res. 2019, 3(2): 165-174.

Striolo, A., Cole, D.R. Understanding shale gas: Recent progress and remaining challenges. Energy Fuels 2017, 31(10): 10300-10310.

Sun, H., Yao, J., Cao, Y., et al. Characterization of gas transport behaviors in shale gas and tight gas reservoirs by digital rock analysis. Int. J. Heat Mass Transf. 2017, 104: 227-239.

Torrie, G.M., Valleau, J.P. Non-physical sampling distributions in monte-carlo free-energy estimation-umbrella sampling. J. Comput. Phys. 1977, 23(2): 187-199.

Vidic, R.D., Brantley, S.L., Vandenbossche, J.M., et al. Impact of shale gas development on regional water quality. Science 2013, 340(6134): 1235009.

Wang, S., Javadpour, F., Feng, Q. Fast mass transport of oil and supercritical carbon dioxide through organic nanopores in shale. Fuel 2016, 181: 741-758.

Yao, J., Sun, H., Huang, Z.Q., et al. Key mechanical problems in the developmentof shale gas reservoirs. Scientia Sinica Physica, Mechanica & Astronomica 2013, 43(12): 1527-1547. (in Chinese)

Yethiraj, A., Striolo, A. Fracking: What can physical chemistry offer? J. Phys. Chem. Lett. 2013, 4(4): 687-690.

Zhao, W.H., Bai, J., Wang, L., et al. Formation of bilayer clathrate hydrates. J. Mater. Chem. A 2015, 3: 5547-5555.

Zhao, W.H., Wang, L., Bai, J., et al. Highly confined water: Two-dimensional ice, amorphous ice, and clathrate hydrates. Acc. Chem. Res. 2014a, 47(8): 2505-2513.

Zhao, W.H., Wang, L., Bai, J., et al. Spontaneous formation of one-dimensional hydrogen gas hydrate in carbon nanotubes. J. Am. Chem. Soc. 2014b, 136(30): 10661-10668.